

# Optical glucose sensing in biological fluids: an overview

Roger J. McNichols\*

Gerard L. Coté

Biomedical Engineering Program  
Texas A&M University  
College Station, Texas 77843-3120

**Abstract.** Recent technological advancements in the photonics industry have led to a resurgence of interest in optical glucose sensing and to realistic progress toward the development of an optical glucose sensor. Such a sensor has the potential to significantly improve the quality of life for the estimated 16 million diabetics in this country by making routine glucose measurements more convenient. Currently over 100 small companies and universities are working to develop noninvasive or minimally invasive glucose sensing technologies, and optical methods play a large role in these efforts. This article reviews many of the recent advances in optical glucose sensing including optical absorption spectroscopy, polarimetry, Raman spectroscopy, and fluorescent glucose sensing. In addition a review of calibration and data processing methods useful for optical techniques is presented.

© 2000 Society of Photo-Optical Instrumentation Engineers. [S1083-3668(00)01401-5]

**Keywords:** glucose sensing, polarimetry raman spectroscopy, infrared absorption, fluorescence.

Paper JBO-90007 received Jan. 25, 1999; revised manuscript received Aug. 3, 1999; accepted for publication Nov. 16, 1999.

## 1 Introduction

It has become overwhelmingly clear that frequent monitoring and tight control of blood sugar levels are requisite for effective management of Diabetes mellitus and reduction of the complications associated with this disease.<sup>1,2</sup> The pain and trouble associated with current “finger-stick” methods for blood glucose monitoring result in decreased patient compliance and a failure to control blood sugar levels. Thus, the development of a convenient noninvasive blood glucose monitor holds the potential to significantly reduce the morbidity and mortality associated with Diabetes.<sup>3–9</sup> The development of such a sensor would also allow automated closed-loop control of cell culture processes which could lead to more efficient and reproducible cell and tissue growth,<sup>10,11</sup> and such a sensor would be useful for on-line process control in the agricultural industry.<sup>12,13</sup>

Recently, renewed interest in, and some significant progress toward, noninvasive optical glucose sensing have come about due, in part, to the unprecedented availability of new technologies. The proliferation of optical communication systems has driven the photonics industry to produce cheap and reliable optical sources, detectors, and imagers, and the availability of powerful computers has made possible the application of extremely complex and powerful data analysis techniques.

Optical glucose measurement techniques are particularly attractive for several reasons: they utilize nonionizing radiation to interrogate the sample, they do not generally require consumable reagents, and they are fast. In this article, theoretical considerations and recent progress in four optical glu-

ucose sensing arenas will be reviewed including: infrared and near-infrared spectroscopy, Raman spectroscopy, polarimetry, and fluorescence spectroscopy. Although optical approaches for glucose sensing are attractive, they are often plagued by a lack of sensitivity and/or specificity since variations in optical measurements depend on variations of many factors in addition to glucose concentration. Isolating those changes which are due to glucose alone and using them to predict glucose concentration is a significant challenge in itself, and to some extent all optical glucose sensing methods rely on solving the so called “calibration problem.” For this reason, this article will also discuss the calibration of optical glucose measurements and the advanced mathematical techniques which have been employed in attacking this hurdle. Finally, conclusions about the near future of optical glucose monitoring will be drawn.

## 2 Review of Diabetes Mellitus

Diabetes mellitus is a chronic systemic disease in which the body either fails to produce or fails to respond to the glucose regulatory hormone insulin. Insulin is required in order for cells to take up glucose from the blood, and in diabetics, a defect in insulin signaling can give rise to large fluctuations in blood glucose levels unless proper management techniques are employed. It is currently estimated that 16 million people in the US and 100 million people world wide suffer from Diabetes mellitus, a disease for which no cure currently exists.<sup>14</sup> Of those afflicted, approximately 5% have what is known as type I diabetes, insulin-dependent diabetes mellitus (IDDM), or juvenile-onset diabetes.<sup>15</sup> Type I diabetes is an autoimmune disease in which the body’s own defenses turn against it and destroy tissue, specifically the insulin-producing

\*The present address of Roger J. McNichols is BioTex, Inc., Bryan, TX.

Address all correspondence to Dr. Gerard L. Coté. Tel: 409-845-4196; Fax: 409-847-9005; E-mail: cote@acs.tamu.edu

**Table 1** Summary of diabetes mellitus.

Type of diabetes	Management strategy	Chronic effects		
		Complication	Treatment	Acute effects
type I Insulin dependent or Juvenile-onset	Routine insulin injections or insulin pump	Vascular disease	none	hyperglycemia leading to ketoacidosis, coma, and death
		Heart disease	Diet	
		Kidney disease (nephropathy) Eye disease (retinopathy)	Dialysis transplant, diet Laser coagulation of neovascularizations	
type II Noninsulin dependent or adult-onset	Diet or oral medications	Anesthesia (neuropathy)	Close attention to wounds—especially foot care	hypoglycemia nausea and weakness
		Poor wound healing	Attention to skin ulcers	

$\beta$  cells of the Islets of Langerhans in the pancreas. The result is an eventual inability to produce insulin. Though not well understood, it is believed that both genetic and viral factors may play a role in this process.<sup>15</sup> The remaining 95% of diabetics suffer from type II diabetes, noninsulin-dependent diabetes mellitus (NIDDM), or adult-onset diabetes. Type II diabetics produce insulin, but for some reason the cells of their bodies do not respond properly to the hormone and fail to take up glucose appropriately. Both types I and II diabetes mellitus can be diagnosed by measuring abnormally high blood glucose levels after a carbohydrate-rich meal.

Associated with diabetes mellitus are a host of secondary complications which conspire to make the disease one of the major killers in the US. Acute effects of diabetes result when blood glucose levels either get too high (hyperglycemia) or too low (hypoglycemia). During hyperglycemia, since the body is unable to use glucose for energy, fats or proteins are metabolized for energy. The metabolism of these substances results in the production of ketone bodies which are toxic in sufficiently high levels and can result in ketoacidosis, coma, and even death. During episodes of hypoglycemia, the body feels weak and because no energy source is available, shock and even coma and death may result.

Chronic complications of diabetes are not well understood, but seem to stem from prolonged hyperglycemia associated with the disease. Effects on the circulatory system and its blood vessels can cause damage to the organs and tissues in the body. Long-term complications of the disease include kidney disease, heart disease, blindness, nerve damage, and gangrene. These effects are not limited to either Type I or II diabetes and, according to the National Institutes of Health, were the source of an estimated 137 billion dollars in associated health care costs in 1995.<sup>14</sup> Table 1 summarizes the management and effects of both types I and II diabetes mellitus.

The goal of diabetes therapy is to approximate the 24 h blood glucose cycle of a normal individual. Accomplishing this goal requires intensive management of blood glucose lev-

els by frequent monitoring of blood glucose and treatment with either diet, medication, or insulin injection. Currently the only available method for monitoring blood glucose requires the acquisition of a small blood sample via a “finger-stick.” This method is inconvenient, messy, painful, and carries a risk of infection, hence patient compliance is often low, and the secondary complications of diabetes are often allowed to progress. One solution to this problem is the development of a painless and convenient noninvasive optical glucose monitor which would allow for fast and frequent measures of blood glucose levels. Many of the proposed techniques rely on secondary indicators of blood glucose such as interstitial fluid glucose, or aqueous humor glucose levels. The development of these devices is further complicated not only by a time lag, but by the physiology of the disease itself. While secondary glucose measures may or may not be well correlated to blood glucose levels in normal individuals, they may be particularly problematic in diabetics. The malfunction of normal glucose transport mechanisms and changes in peripheral vasculature are problems for many secondary measures, especially since the progressive nature of the disease means that these relationships may be changing with time. Given this, it is important to insure that a noninvasive glucose sensor works in diabetic patients with abnormal physiology as well as in normal patients.

### 3 Optical Absorption Techniques

Optical absorption techniques for quantification of glucose are based on selective absorption of light by the molecule which is described by the Beer–Lambert law:

$$I = I_0 e^{-\epsilon CL}$$

Here  $I_0$  is the intensity of incident optical radiation,  $I$  is the transmitted intensity,  $\epsilon$  is the molar extinction coefficient in  $(\text{mol/L})^{-1} \text{cm}^{-1}$  (and is dependent on wavelength),  $C$  is the molar concentration, and  $L$  is the pathlength in cm. Measure-

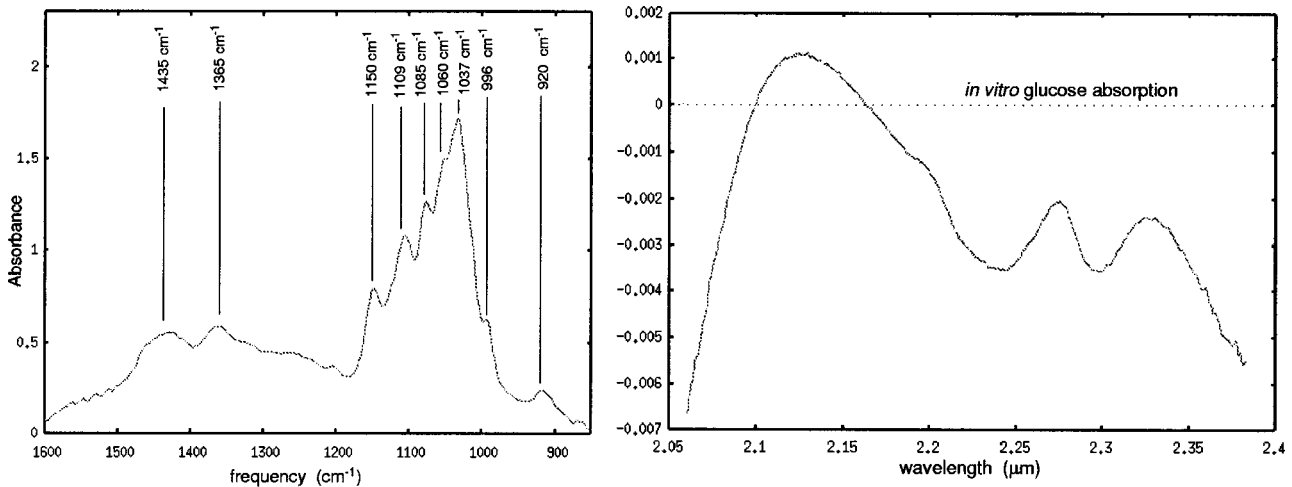


**Fig. 1** Optical absorption spectra for glucose. (a) Midinfrared region extending from 1600 to 900  $\text{cm}^{-1}$  or 6.25 to 11  $\mu\text{m}$  and showing absorption peak assignments. (b) Near-infrared region extending from 2.0 to 2.5  $\mu\text{m}$  or 5000 to 4000  $\text{cm}^{-1}$ . Note that the magnitude of the three absorbance peaks in the NIR region is much smaller.

ments are generally reported in absorbance,  $A = \log(I_0/I)$ , such that the absorbance of several species is additive. Optical absorption spectroscopy for glucose quantification has generally been restricted to either the midinfrared (MIR) or the near-infrared (NIR) spectral region. Figure 1 shows examples of both MIR and NIR optical absorption spectra for aqueous glucose after water subtraction.

The MIR region of the spectrum ranges from 2.5 to 50  $\mu\text{m}$  (4000–200  $\text{cm}^{-1}$ ), and it is in this region that absorption bands due to fundamental stretching and bending modes of the molecule may be seen. For this reason, spectroscopy in the MIR or “finger-print” region is extremely useful for spectral identification of compounds. However, the magnitude of background absorption bands due to solution constituents like water severely limits the path length which can be used in MIR transmission spectroscopy to a few hundred microns or less.

Transmission spectroscopy in the MIR region as a means for quantifying glucose has been explored by Zeller et al. who used a MIR spectrophotometer and glucose doped whole blood in a 25  $\mu\text{m}$  ZnSe transmission cell to analyze several glucose peaks between 8.5 and 9  $\mu\text{m}$  (1175–1110  $\text{cm}^{-1}$ ).<sup>16</sup> Bhandare et al. also investigated the MIR using transmission spectrophotometry of phosphate buffer solutions containing glucose and several other interfering components in order to compare the effectiveness of single peak calibration, principal component regression analysis, partial least squares regression analysis, and artificial neural networks.<sup>8,17</sup> Attenuated total reflection (ATR) MIR spectroscopy, a technique in which a specialized crystal is used to probe the superficial surface layers of a sample, has also been suggested as a means for quantifying blood glucose and has been investigated by Heise et al. in whole blood.<sup>18</sup> Finally, Optiscan, Inc. has reported using MIR spectroscopic measurements of glucose made with the body’s own heat emission as the MIR source.<sup>19</sup>

In contrast to the MIR region, the NIR region of the spectrum, which extends from 700 to 2500 nm (14 000–4000  $\text{cm}^{-1}$ ), contains little specific information. Absorption bands in this region are due to overtone vibrations of anharmonic

fundamental absorption bands or to combinations of fundamental absorption bands primarily associated with C–H, O–H, and N–H stretching vibrations. For overtone vibrations, it is usually only the first, second, and third overtones that are seen, with the magnitude of the absorption peak diminishing substantially with overtone order. As mentioned, these absorption bands are broad, are easily influenced by hydrogen bonding and temperature effects, and demonstrate substantial overlap. Nonetheless, the region is attractive for quantitative spectroscopy since NIR instrumentation is readily available and the reduced absorption magnitude allows the use of reasonably large path lengths. An excellent review of the theory and assignment of NIR absorption bands can be found in Refs. 20 and 21 and has more recently been presented in Refs. 12 and 22.

Noninvasive quantification of blood glucose using the very NIR region (700–1300 nm) was originally suggested by Rosenthal who proposed to use NIR transmission spectroscopy through the fingertip.<sup>3,23</sup> Robinson et al. combined NIR spectroscopy in this same wavelength region with partial least-squares (PLS) analysis and claimed noninvasive glucose prediction through the finger with an accuracy of 20 mg/dL in diabetic patients.<sup>9</sup> More recently, Danzer et al. used diffuse reflectance spectroscopy in this region and demonstrated a predictive error of 36 mg/dL.<sup>24</sup> Although specific glucose spectral peaks are hard to identify in this region of the spectrum, particularly at physiological concentrations, it remains popular with researchers because relatively inexpensive optical detectors and components can potentially be used.

The near-infrared region which lies between 2.0 and 2.5  $\mu\text{m}$  has become increasingly popular for aqueous glucose measurements. This region contains a relative minimum in the water absorption spectrum and readily identifiable glucose peak information. This region has been utilized by Haaland et al. in an attempt to quantify glucose *in vitro* in whole blood<sup>25</sup> and by Marbach et al. who used diffuse reflectance spectroscopy of the human lip in an attempt to measure glucose *in vivo*.<sup>26</sup> Arnold et al. have demonstrated that the application of Fourier filtering techniques to spectral data from this

region is effective for quantifying aqueous glucose<sup>27–29</sup> and that digital filtering may also be used to correct for the temperature sensitivity of the NIR spectrum.<sup>30</sup> Since this initial interest, several groups have demonstrated moderate success with this spectral region in quantifying aqueous glucose concentrations of *in vitro* phantoms of various complexity including Shengtian et al.<sup>31</sup> who used fat, protein, and glucose phantoms, Chung et al.<sup>32</sup> who used mixtures of glucose, glutamine, ammonia, lactate, and glutamate to simulate cell culture media, Mattu et al.<sup>33</sup> who used phantom solutions of bovine serum albumin doped with glucose, and McShane et al.<sup>34</sup> who have been able to quantify glucose, lactate, and ammonia in cell culture media obtained from fibroblast cultures. Each of these investigators utilized NIR spectroscopy measurements in the 2.0–2.5  $\mu\text{m}$  spectral region coupled with PLS multivariate calibration techniques which are described later in this article. Sensing sites proposed for NIR measurements include the fingertip,<sup>9,23,24</sup> the earlobe,<sup>19</sup> the tongue,<sup>19</sup> the lip,<sup>35</sup> and the forearm.<sup>19,36</sup>

Glucose sensing using near infrared spectroscopy is by no means a simple problem. Glucose absorption peaks whose magnitude is relatively small compared to a large aqueous background spectrum often yield low signal-to-noise measurements. NIR spectral measurements are further plagued by a lack of repeatability. Near infrared spectra are sensitive to a host of factors including temperature, *pH*, and scattering. Additionally, *in vivo* measurements may be susceptible to differences in skin pigmentation, hydration, blood flow, probe placement, and probe pressure. Finally, it should be noted that the NIR spectrum of glucose is very similar to that of other sugars<sup>37</sup> including, in particular, fructose which is often used by diabetics as an alternative to glucose. Despite these difficulties, however, near infrared methods have demonstrated significant promise in becoming a viable technique for noninvasive glucose sensing.

#### 4 Polarimetry

Polarimetric quantification of glucose is based on the phenomenon of optical rotatory dispersion (ORD) whereby a chiral molecule in an aqueous solution will rotate the plane of linearly polarized light passing through the solution. This rotation is due to a difference in the indices of refraction  $n_L$  and  $n_R$  for left- and right-circularly polarized light passing through a solution containing the molecule. It occurs by virtue of the molecule's chirality or "handedness" by which we mean the molecule has at least one center about which its mirror image cannot be superimposed upon itself. In such a case, random orientation of molecules in solution will result in a bulk difference in  $n_L$  and  $n_R$  for the solution, and the resultant phase shift between left- and right-circularly polarized waves gives rise to a rotation of plane polarized light passing through the solution. The angle of rotation depends linearly on the concentration of the chiral species, the pathlength through the sample, and a constant for the molecule called the specific rotation. The net rotation is expressed as  $\phi = \alpha_\lambda LC$ , where  $\alpha_\lambda$  is the specific rotation for the species in  $^\circ\text{dm}^{-1}(\text{g/L})^{-1}$  at wavelength  $\lambda$ ,  $L$  is the pathlength in dm, and  $C$  is the concentration in g/L. Glucose in the body is dextrorotatory (rotates light in the right-handed direction) and has a specific rotation of  $+52.6^\circ\text{dm}^{-1}(\text{g/L})^{-1}$  at the sodium *D*-line

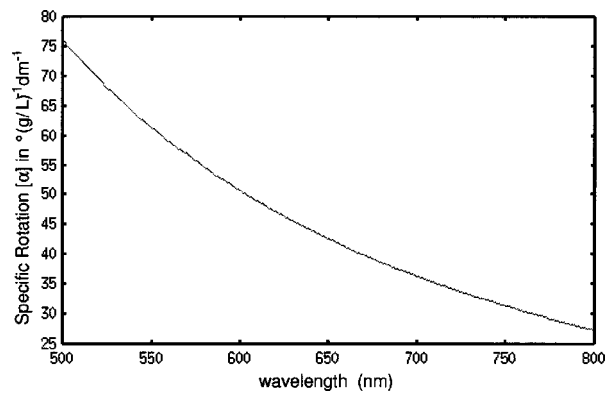


**Fig. 2** Optical rotatory dispersion (ORD) curve for glucose. The specific rotation in  $^\circ(\text{g/L})^{-1} \text{dm}^{-1}$  is shown vs wavelength in nm. Adapted from Ref. 39.

of 589 nm.<sup>38</sup> Figure 2 is an ORD curve for glucose showing specific rotation versus wavelength for light in the visible to near-infrared range.

At physiological concentrations and pathlengths of about 1 cm, optical rotations due to glucose are on the order of 5 millidegrees. A number of techniques for obtaining measurements with this high degree of accuracy exist and generally fall into two categories: those which utilize crossed polarizers to measure rotation via amplitude changes,<sup>39–41</sup> and those which measure the relative phase shift of modulated polarized light passing through the sample.<sup>42,43</sup> Figure 3 illustrates each of these approaches schematically. Figures 3(a) and 3(c) represent optical systems for polarimetry based on the amplitude and phase techniques, respectively. Figures 3(b) and 3(d) illustrate the resulting polarization and intensity signals which contain optical rotation information.

Advantages of polarimetric glucose sensing methods include the use of readily available visible sources, the concomitant ability to use substantial path lengths in aqueous solutions, and the prospect of miniaturizing the optical components required. Because skin tissue is a highly scattering medium, noninvasive measurements through the skin are generally plagued by a high degree of depolarization and a loss in signal-to-noise. Even for red light, scattering is such that a tissue thickness of 4 mm is sufficient to cause  $\sim 95\%$  depolarization.<sup>44</sup> For this reason, a number of investigators have suggested the anterior chamber of the eye (the fluid-filled space directly below the cornea) as a sight well suited for polarimetric measurements since scatter in the eye is generally very small compared to other tissues. Figure 4 illustrates one commonly proposed optical sensing path. The anterior chamber is filled with a fluid called the aqueous humor which Pohjola reports has an age-dependent steady-state glucose concentration about 70% that of blood.<sup>45</sup> A time-lag on the order of minutes between blood and aqueous humor glucose concentrations has been reported by March et al. who performed *in vivo* measurements on rabbits.<sup>46,47</sup> More recently it has been suggested that this time-lag may actually take 30 min as reported by Chou et al.<sup>48</sup> While quantification of the aqueous humor glucose time-lag in humans has not been reported, algorithms that can compensate for a time delay and

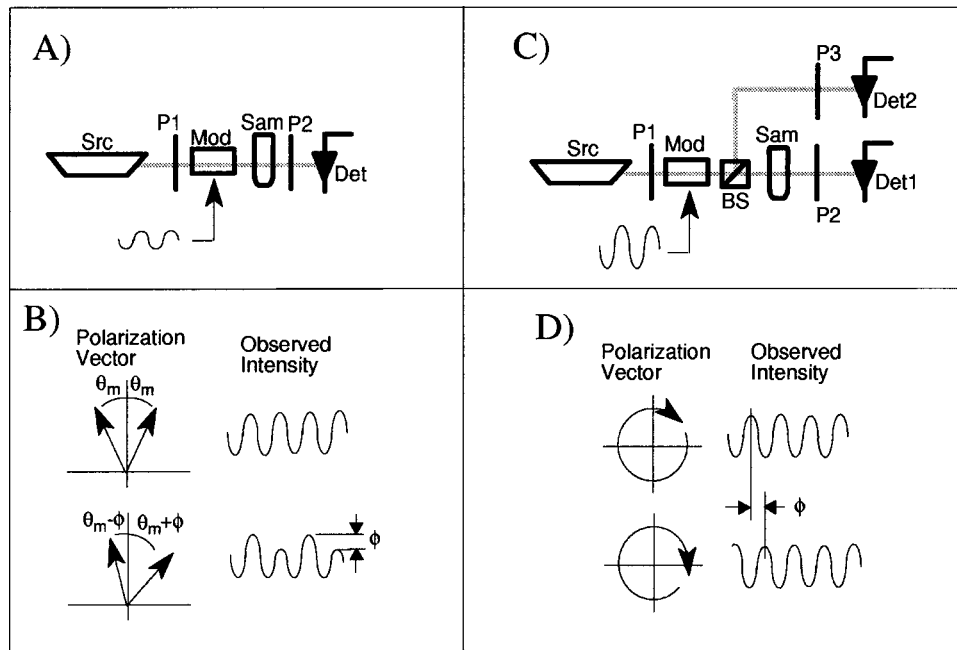


**Fig. 3** Amplitude and phase based polarimetry measurements. (a) In the amplitude approach light from a monochromatic source (Src) is passed through a linear polarizer (P1), a polarization modulator (Mod), a sample (Sam), and a second linear polarizer perpendicular to the first (P2) before being recorded by a detector (Det). (b) The resulting polarization vector and observed intensity are symmetric when no optically active sample is present and asymmetric if the sample is optically active with net rotation  $\phi$ . (c) In the phase approach, polarization modulated sample and reference beams are split by a beam splitter (BS), passed through crossed linear polarizers (P2, P3), and recorded by separate detectors (Det1, Det2). (d) A rotation of polarization by the sample causes a phase shift between the intensity signals recorded by the two detectors.

predict glucose levels in near-real-time may need to be developed.

March was the first to suggest optical glucose measurements in the eye using an open-loop, amplitude based polarimeter.<sup>46</sup> Coté later developed a phase measurement polarimeter in order to increase the signal-to-noise of the polarimetry measurement which he demonstrated *in vitro*.<sup>42</sup> Goetz used an amplitude-based design and improved upon it by

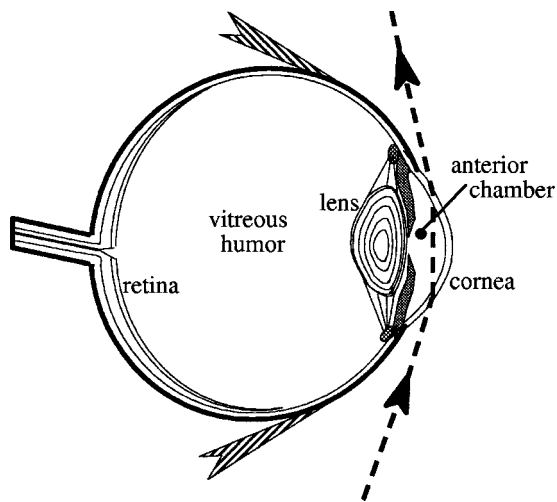


**Fig. 4** Optical sensing in the anterior chamber of the eye. Light passing through the anterior chamber of the eye interacts with the aqueous humor. A commonly proposed beam path is shown.

implementing a closed-loop feedback control which increased stability of the optical measurement<sup>39</sup> and demonstrated *in vitro* sensitivity on the order of a few millidegrees. Cameron later adapted this system to use digital feedback control in order to further increase the robustness and stability of the system<sup>49</sup> and demonstrated measurement of glucose in aqueous cell culture media.<sup>50</sup> King et al. have utilized an amplitude-based approach in which the two polarization modulators required in the systems of Goetz and Cameron were replaced by a single Pockel's cell.<sup>51</sup>

Potential problems with polarimetric glucose sensing in the eye include optical rotation due to the cornea, birefringence of the cornea, the presence of other optically active confounders (for example ascorbate, albumin, and the aforementioned fructose) in the aqueous humor, and saccadic motion artifacts which could give rise to pathlength fluctuations. Problems related to corneal rotation and rotations due to other confounders could potentially be solved by using multiple wavelengths for polarimetric measurements since optical rotations due to multiple species exhibit linear superposition.<sup>52,53</sup> King et al. demonstrated *in vitro* elimination of confounders using a multiwavelength system with two HeNe lasers at 594 and 633 nm,<sup>51</sup> and more recently Coté et al. have used diode lasers at 670 and 830 nm in a digital closed-loop system.<sup>54</sup> The problem of corneal birefringence might be suitably addressed with the use of appropriate optics<sup>46</sup> or by using multiple wavelengths. Alternatively, a polarization system designed to extract the full Jones or Mueller matrix for the system could be used to separate out specific rotation from birefringence.<sup>55</sup>

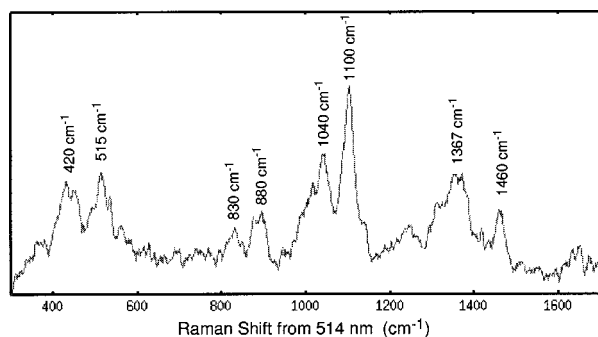


**Fig. 5** Typical Raman spectrum for aqueous glucose. The Stokes Raman spectrum is shown as vibrational intensity vs shift in wave numbers from 514 nm excitation wavelength. The water background has been subtracted.

## 5 Raman Spectroscopy

Raman spectra are observed when incident light at frequency  $\nu_0 = c/\lambda_0$  is inelastically scattered at frequencies  $\nu_0 \pm \nu_i$ . The loss (Stokes shift) or gain (anti-Stokes shift) of photon energy, and hence frequency, is due to transitions of the rotational and vibrational energy states within the scattering molecule. The observed shifts  $\nu_i$  are independent of the excitation frequency  $\nu_0$  and provide specific information about the chemical structure of the sample. Since the Raman spectrum is independent of excitation frequency, an excitation frequency may be chosen which is appropriate for a particular sample. It is important to note, however, that the intensity of Raman scattered peaks generally falls off with decreasing frequency as a function of  $\nu_0^4$ .

Raman spectroscopy has been used extensively as a tool for studying molecules of fundamental biological importance<sup>56</sup> and has been reviewed thoroughly as a tool for cancer detection.<sup>57</sup> Like infrared absorption spectra, Raman spectra exhibit highly specific bands which are dependent on concentration. However, in the Raman case, overtone and combination bands are much weaker making spectra simpler, and the Raman spectrum of water is fairly weak which makes aqueous spectroscopy possible. On the other hand, the Raman signal itself is weak and it is only with the recent availability of highly sensitive charge-coupled device (CCD) arrays that quantitative Raman spectroscopy of physiological glucose solutions has become feasible. While the increased availability and affordability of laser sources and detection systems for Raman spectroscopy make the technique an important contender in the glucose sensing arena, development of a Raman based glucose sensor also faces some large hurdles. A primary drawback is the fact that scatter and reabsorption in biological tissues make detection of Raman shifts due to physiological concentrations difficult. For this reason, several investigators have suggested the anterior chamber of the eye and the aqueous humor as a sensing site for Raman spectroscopy.<sup>58–61</sup> However, the power of laser irradiation required does pose a safety concern. Further, background fluorescence signals, which are often as large or larger than the Raman signal itself, are also a problem in biological media where proteins are present.<sup>57</sup> Use of longer excitation wavelengths can circumvent this problem to some extent, but the intensity of the Raman signal falls off dramatically as excitation wavelength

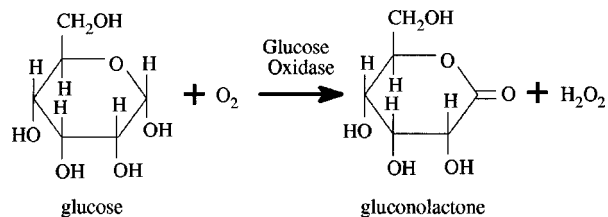


**Fig. 6** The oxidation of glucose by glucose oxidase. Glucose and diatomic oxygen are consumed to form a gluconolactone and hydrogen peroxide.

is increased. Figure 5 shows a Raman spectrum and some peak assignments for aqueous glucose excited by 514 nm argon ion laser light.

Examples of Raman spectroscopy for glucose quantification include work by Wang et al. who used water subtraction techniques to extract and quantify the glucose doublet shift at  $2900\text{ cm}^{-1}$  in the presence of other confounders,<sup>61</sup> work by Goetz et al. who applied multivariate PLS regression to Raman spectra from aqueous mixtures containing glucose and other metabolites,<sup>62</sup> work by Wickstead et al. who used Raman spectroscopy to quantify glucose in aqueous humor samples,<sup>58</sup> and work by Berger et al.<sup>63</sup> and Lambert et al.<sup>64</sup> who have applied PLS analysis to aqueous solutions containing glucose and biological confounders. Dou et al. have also presented measurement of glucose in water using a compact system which uses a semiconductor laser and a band-pass filter to measure the intensity of a single Raman band.<sup>65</sup> Tarr et al. have proposed the use of stimulated Raman emission (a technique in which a second “probe” beam separated in frequency from the main excitatory pump beam by a Stokes shift is used to enhance a single Raman resonance) for detection of glucose in the aqueous humor of the eye.<sup>59,66</sup> As in the case of NIR spectroscopic quantification, the emergence and computational accessibility of PLS and powerful preprocessing methods is increasing the quantitative ability of Raman spectroscopy. Berger et al. have demonstrated that incorporation of pure component spectra into the calibration model is useful for quantitative Raman spectroscopy<sup>67</sup> and Spiegelman et al. have demonstrated the power of wavelength selection routines on Raman spectra of aqueous glucose solutions.<sup>68</sup>

## 6 Fluorescent Techniques

A number of novel fluorescence-based techniques for glucose sensing have been presented. Those which seem to have demonstrated the most promise generally fall into two categories: the glucose-oxidase based sensors and the affinity-binding sensors. Sensors in the first category use the electroenzymatic oxidation of glucose by glucose-oxidase (GOX) in order to generate an optically detectable glucose-dependent signal. The oxidation of glucose and oxygen to form gluconolactone and hydrogen peroxide is illustrated in Figure 6.

Several methods for optically detecting the products of this reaction and hence the concentration of glucose driving the reaction have been devised. Since oxygen is consumed in the reaction at a rate dependent on the local concentration of glucose, a fluorophore which is sensitive to local oxygen concentration can also be used to quantify glucose concentration. For example, Schaffar and Wolfbeis immobilized GOX onto the

end of a luminescence oxygen optrode in order to create a sensor whose luminescence was dependent on glucose concentration.<sup>69</sup> Moreno-Bondi et al. have presented an optical fiber glucose sensor created by attaching GOX to an oxygen sensor based on the dynamic quenching of the luminescence of tris(1,10-phenanthroline)-ruthenium(II) cation by molecular oxygen.<sup>70</sup> More recently, Rosenzweig and Kopelman have improved the sensitivity of this glucose optrode by using a photopolymerization process to incorporate GOX and the oxygen indicator, onto the end of a small diameter optical fiber.<sup>71</sup> One drawback to GOX based sensors is that their response depends not only on glucose concentration but on local oxygen tension as well. Li et al. have proposed a dual fiber-optic fluorescence sensor which incorporates oxygen sensing into a GOX based fluorescent sensor.<sup>72</sup> Fluorescence quenching of a Ruthenium dye by oxygen is measured at two chemistry sites one of which contains GOX and hence decreased quenching depending on the concentration of glucose. The sensing sites are affixed to the end of an imaging fiber-bundle and a CCD camera is used to simultaneously measure fluorescence at each site.<sup>72</sup>

Other more elaborate GOX based fluorescent sensors have also been proposed. For example, Gungsingham et al. used the redox mediator tetrathiafulvalene (TTF) whose oxidized form TTF<sup>+</sup> reacts with the reduced form of GOX to reversibly form TTF<sup>0</sup>. Since TTF<sup>+</sup> absorbs in the 540–580 nm range, a means for quantifying the presence of TTF<sup>+</sup> (and hence glucose driving the production of reduced GOX) is available.<sup>73</sup> Abdel-Latif et al. have used a scheme in which hydrogen peroxide (H<sub>2</sub>O<sub>2</sub>) generated from the GOX reaction with glucose reacts with bis(2,4,6-trichlorophenyl) oxalate (TCPO) to form a peroxyoxylate.<sup>74</sup> In this approach, the peroxyoxylate formed transfers chemiluminescent energy to an accepting fluorophore which in turn emits photons at a characteristic wavelength. The emission by the fluorophore is proportional to glucose concentration and can be detected optically.<sup>74</sup>

Fluorescent affinity-binding sensors utilize competitive binding between glucose and a suitably labeled fluorescent compound to a common receptor site. In initial work by Shultz et al. immobilized concanavalin A (ConA) was used as a receptor for competing species of fluorescein isothiocyanate (FITC) labeled dextran and glucose.<sup>75,76</sup> Increased concentrations of glucose displace FITC-dextran from ConA sites thus increasing the concentration and fluorescence intensity of FITC-dextran in the visible field. In more recent work, this group and others have exploited the phenomenon of fluorescence resonance energy transfer (FRET) whereby an acceptor in close proximity to a fluorescent donor can induce fluorescence quenching in the latter. In one scheme, a tetramethylrhodamine isothiocyanate (TRITC) label is added to the ConA which causes quenching of bound FITC-dextran. Increasing glucose concentration causes increased FITC-dextran displacement and, hence, higher FITC fluorescence intensity.<sup>77</sup> In another approach, these investigators have used FRET between rhodamine-labeled dextran and FITC-labeled dextran molecules bound to multiple receptor sites on the same ConA molecule as a means of quantifying glucose by the resulting increase in FITC fluorescence caused by the presence of glucose.<sup>78</sup> Lackowicz et al. used phase-modulation fluorimetry and FRET based dextran/ConA affinity sensor in order to increase the reliability of absolute fluorescence

measurements,<sup>79</sup> and have more recently devised a similar sensor in which ruthenium-ConA and maltose-insulin-malachite green (MIMG) are used as the reagents. Increased glucose concentration causes an increase in both fluorescence intensity and fluorescence lifetime of the ruthenium dye.<sup>80</sup> In general, fluorescence sensors offer the advantage that can be made highly specific to glucose and eliminate many of the potential interferences common with other techniques. However, they suffer the serious drawback that in all cases exogenous chemistry is required which must be introduced to the body or sample. Additionally, this chemistry may be susceptible to degradation over time via consumption, photobleaching, or denaturation.

## 7 Calibration Of Optical Measurements

In its simplest form, the calibration problem for optical glucose measurement can be stated: given a set of many optical measurements and corresponding glucose concentrations, develop a model which will allow prediction of glucose concentration based on analysis of future similar optical measurements. Though attempts at univariate regression analysis for single-wavelength prediction of glucose have been made,<sup>16,23</sup> it is well established that such methods are of little use in complex biological media where several varying components with overlapping spectral features exist. In such a case, multivariate calibration methods are employed which use multiple measurements at each particular glucose concentration to eliminate the effects of confounders. Several of these methods are based on a least squares solution to the multivariate calibration problem and will be discussed briefly here in the context of glucose quantification. Excellent sources of information on the formulation and application of multivariate calibration statistics to optical spectroscopic data may be found in McClure,<sup>81</sup> Martens and Næs,<sup>82</sup> Heise and Marbach,<sup>18</sup> Burns and Ciurczak,<sup>22</sup> or Haaland and Thomas.<sup>83</sup>

The simplest approach for applying multivariate calibration techniques to spectral data is the so-called classical least-squares (CLS) or **K**-matrix approach. In this formulation, observed spectra are assumed to be measured responses to known concentrations of  $p$  analytes:  $\mathbf{A} = \mathbf{K}\mathbf{C}$  where  $\mathbf{A}$  is the  $m \times n$  matrix of  $m$ -point column spectra for  $n$  samples,  $\mathbf{C}$  is the  $p \times n$  matrix of concentrations for  $p$  analytes in  $n$  samples, and  $\mathbf{K}$  is the  $m \times p$  matrix relating observed absorbance at each wavelength to analyte concentration. As an example, consider the simplest case for one analyte and two spectral measurements at two wavelengths.

The problem can be represented by the following equation:

$$\begin{bmatrix} A_1^{\lambda_1} & A_2^{\lambda_1} \\ A_1^{\lambda_2} & A_2^{\lambda_2} \end{bmatrix} = \begin{bmatrix} k_{\lambda_1} \\ k_{\lambda_2} \end{bmatrix} [c_1 \quad c_2],$$

where  $A$  values represent the observed absorption at each wavelength for each known concentration  $c$ , and the  $k$  values are the unknown model parameters relating absorbance to analyte concentration. In this case, postmultiplying both sides by  $\mathbf{C}^T = [c_1 \ c_2]^T$  and then postmultiplying both sides by the inverse of  $\mathbf{C}\mathbf{C}^T$  (which is guaranteed to be nonsingular when the columns of  $\mathbf{C}$  are linearly independent) yields a solution for  $\mathbf{K}$ :

$$\mathbf{K} = \begin{bmatrix} k_{\lambda_1} \\ k_{\lambda_2} \end{bmatrix} = \begin{bmatrix} A_1^{\lambda_1} c_1 + A_2^{\lambda_1} c_2 \\ A_1^{\lambda_2} c_1 + A_2^{\lambda_2} c_2 \end{bmatrix} \frac{1}{c_1^2 + c_2^2}.$$

For subsequent measurements we reformulate the problem to calculate an estimator of  $c$  from a new spectrum  $A_*$  and the model response matrix  $\mathbf{K}$ . In this simple case we can write (using the same procedure as above):

$$\hat{c} = \frac{k_{\lambda_1} A_*^{\lambda_1} + k_{\lambda_2} A_*^{\lambda_2}}{k_{\lambda_1}^2 + k_{\lambda_2}^2}.$$

In the overdetermined case where  $n > p$ , the least-squares model solution for  $\mathbf{K}$  is found from the response matrix and the pseudoinverse of the concentration matrix  $\mathbf{K} = \mathbf{A}\mathbf{C}^T(\mathbf{C}\mathbf{C}^T)^{-1}$ ; concentrations of subsequently analyzed mixtures are predicted as

$$\hat{\mathbf{c}} = (\mathbf{K}^T\mathbf{K})^{-1}\mathbf{K}^T\mathbf{a}.$$

In this case, exact knowledge of the analyte concentrations in the calibration standards is assumed and all error is attributed to the measured responses. In the case of optical spectroscopy in biological samples, this is not a particularly valid assumption since spectral measurements with a high signal-to-noise are possible, but analysis of calibration samples is often impractical or prone to significant error. An alternate formulation proposed by Brown et al.<sup>84</sup> is to assume that the measured responses are accurate and all errors are found in the matrix of calibration concentrations. This so-called inverse least-squares (ILS) or  $\mathbf{P}$ -matrix approach is formulated:  $\mathbf{C} = \mathbf{A}^T\mathbf{P}$ , where  $\mathbf{C}$  and  $\mathbf{A}$  are as before and  $\mathbf{P}$  is now the sensitivity matrix for the inverse problem. The prediction model for subsequent observations is

$$\hat{\mathbf{c}}^T = \mathbf{a}^T[(\mathbf{A}\mathbf{A}^T)^{-1}\mathbf{A}\mathbf{C}].$$

This approach is difficult to implement in practice, however, since well-conditioned solutions require an orthogonal set of calibration mixtures and restrictions on the number of spectral wavelengths which may be used.<sup>83,84</sup>

In an attempt to overcome the limitations of both of these methods, Wold et al. suggested the technique of partial least-squares (PLS) regression.<sup>85</sup> Originally developed as a method for modeling complex econometric data, PLS has become overwhelmingly popular in optical spectroscopy and chemometric analysis. PLS regression is similar to principal component regression (PCR) in that matrix decomposition techniques are used to model the response matrix  $\mathbf{A}$ . However, in PLS, this decomposition is combined with a regression model which attempts to optimize correlation with the concentration matrix  $\mathbf{C}$ . In PLS, observations in  $\mathbf{A}$  are decomposed into a number of latent variables or ‘‘factors’’ which are then used as predictors in the regression model. Increasing the number of factors used allows for modeling of more complex solutions with multiple varying components, while reduction in the number of factors helps to filter spectral noise and prevent over fitting of the data. One way to perform this analysis is to use a form of singular value decomposition (SVD). This method can be illustrated for a single analyte as follows. First assume that the measured spectral response to several solutions with known concentrations of a single analyte are con-

tained in the columns of the response matrix  $\mathbf{A}$  and that the corresponding concentrations reside in the row vector  $\mathbf{c}$ .  $A_{ij}$  is the measured response at the  $i$ th wavelength due to the analyte concentration  $c_j$ .

$$\mathbf{A} = \begin{bmatrix} A_{11} & A_{12} & A_{13} \\ A_{21} & A_{22} & A_{23} \\ A_{31} & A_{32} & A_{33} \\ A_{41} & A_{42} & A_{43} \end{bmatrix} \quad \mathbf{c} = [c_1 \quad c_2 \quad c_3].$$

We then wish to formulate a predictive model relating  $\mathbf{c}$  to  $\mathbf{A}$ . The matrix  $\mathbf{A}^T\mathbf{A}$  is guaranteed to be full-rank and this is used to formulate the pseudoinverse in the ILS approach. However,  $\mathbf{A}$  may contain substantial noise, such that the condition number of  $\mathbf{A}^T\mathbf{A}$  is not good, and much of the variation in  $\mathbf{c}$  may be described by a few trends or factors in  $\mathbf{A}$ . The matrix  $\mathbf{A}$  can always be rewritten using a singular value decomposition.<sup>86</sup>

$$\mathbf{A} = \mathbf{U}\mathbf{\Sigma}\mathbf{V}^T = \mathbf{U} \begin{bmatrix} \sigma_1 & 0 & 0 \\ 0 & \sigma_2 & 0 \\ 0 & 0 & \sigma_3 \\ 0 & 0 & 0 \end{bmatrix} \mathbf{V}^T,$$

where  $\mathbf{U}$  is a  $m \times m$  (in this case  $4 \times 4$ ) orthogonal matrix called the left singular values (LSV) matrix,  $\mathbf{V}$  is an  $n \times n$  (in this case  $3 \times 3$ ) orthogonal matrix called the right singular values (RSV) matrix, and  $\mathbf{\Sigma}$  is an  $m \times n$  matrix with off diagonal elements equal to zero and  $\sigma_1 \geq \sigma_2 \geq \dots \sigma_n \geq 0$ . One of the features of PLS is that information from the  $\mathbf{c}$  matrix is utilized in the singular value decomposition as well, and the SVD is iteratively performed on the covariance matrix  $\mathbf{c}\mathbf{A}^T\mathbf{A}\mathbf{c}^T$  such that the resulting  $\mathbf{\Sigma}$  matrix is upper triangular. In this case, the decomposition represents an eigenvalue decomposition of the  $\mathbf{A}$  matrix with respect to the concentration matrix.

In PLS parlance, the LSV matrix  $\mathbf{U}$  is the ‘‘PLS loading’’ matrix and can be used to calculate the ‘‘PLS scores’’ matrix  $\mathbf{T} = \mathbf{U}\mathbf{A}$ . The scores and loading matrices are then used to reconstruct an estimator of the original  $\mathbf{A}$  matrix which should contain only the variations most relevant to the variation in  $\mathbf{c}$ :

$$\tilde{\mathbf{A}} = \mathbf{U}^T\mathbf{T} = \mathbf{U}^T\mathbf{U}\mathbf{A}.$$

If the full  $\mathbf{U}$  and  $\mathbf{T}$  matrices are used, the reconstruction should be exact, however, in PLS, usually only the first several rows of these matrices are used and  $\tilde{\mathbf{A}}$  is an estimate of  $\mathbf{A}$ . The number of rows of  $\mathbf{U}$  and  $\mathbf{T}$  which are used to produce this estimator is termed the number of factors included in the model. It should be noted that for row spectra, the roles of  $\mathbf{U}$  and  $\mathbf{V}$  are reversed. The PLS regression coefficients for the model are calculated by

$$\mathbf{b} = \mathbf{V}(\mathbf{\Sigma}^{-1})\mathbf{U}^T\mathbf{c},$$

where again the number of rows of  $\mathbf{U}$  and  $\mathbf{V}$  used are the number of factors included in the model. Finally, we come up with the estimates for concentration as:

$$\hat{\mathbf{c}} = \tilde{\mathbf{A}}\mathbf{b}.$$

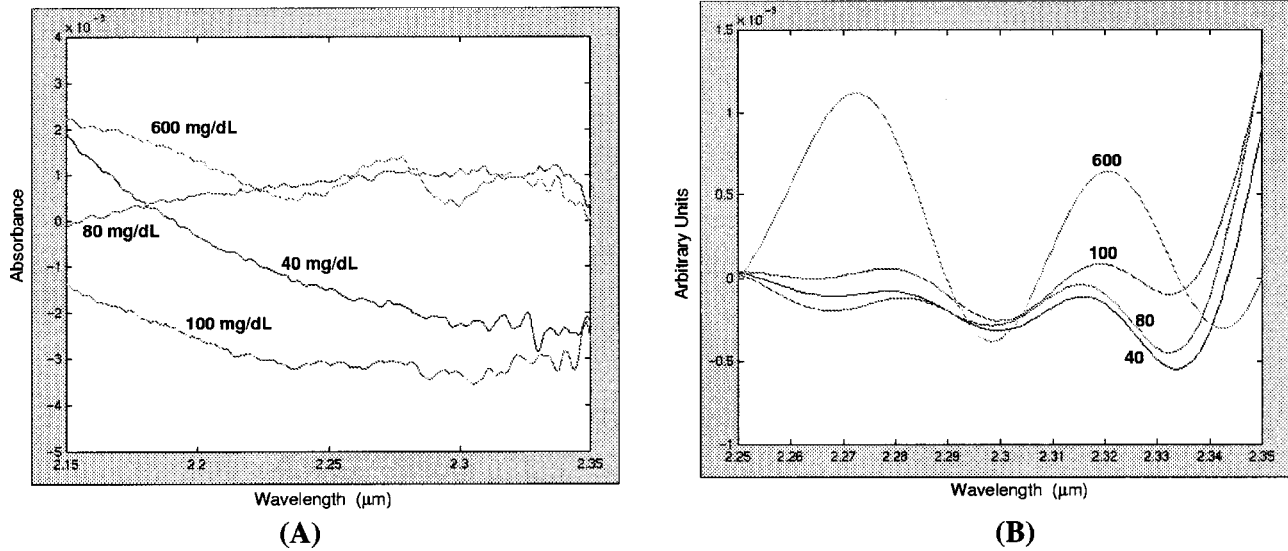


**Fig. 7** NIR spectra of aqueous glucose solutions before (a) and after (b) application of Fourier filtering. The filter has the effect of enhancing glucose specific information by removing baseline offsets and high frequency noise. Adapted from Ref. 96.

The inclusion of more factors makes the reconstructed  $\tilde{\mathbf{A}}$  matrix closer to  $\mathbf{A}$  and hence may fit the calibration data better. Alternatively, reducing the number of factors used to construct  $\tilde{\mathbf{A}}$  decreases the influence of noise and may result in a more stable model which is less prone to over fitting of calibration data. Judicious selection of latent variables is key to the success of the PLS technique and has been the object of several articles.<sup>68,87–89</sup>

Recently, PLS methods have become particularly powerful due to their combination with complex spectral data preprocessing routines such as multiplicative scalar correction (MSC),<sup>90</sup> Fourier filtering techniques,<sup>27–30,33,88,91,92</sup> and time-domain filtering,<sup>93</sup> to name a few. Of particular note is the development of filter optimization routines which depend on the iterative search for spectral filter parameters which optimize the results of the PLS calibration model.<sup>28,93,94</sup> While the use of Fourier transform filtering and reconstruction of spectra was first introduced by McClure et al., its use was primarily intended as a means of data reduction.<sup>95</sup> Coupling of iterative filter optimization routines and PLS is extremely computation intensive, and only recently has the availability of high-end computational platforms led to wide spread use of this technique.<sup>26,27,28,92–94</sup>

Figures 7(a) and 7(b) illustrate the power of Fourier filtering in the preprocessing of data. Figure 7(a) shows water subtracted NIR spectra for several aqueous glucose solutions collected with a fiber-optic probe. Baseline shifts and noise make identification of glucose absorption bands impossible in all but the highest concentration spectra. [Compare these to the spectrum in Figure 1(b).] Figure 7(b) shows the same spectra after Fourier filtering. The filter has the effect of enhancing glucose specific information by removing baseline offsets and high frequency noise. The design and use of digital filters for preprocessing of spectra has been presented by Arnold and Small,<sup>27,28</sup> McShane,<sup>68,88</sup> and others.<sup>30–33,94</sup>

Another family of popular spectroscopy calibration tools are the so-called “wavelength selection” algorithms. The

purpose of these techniques is to reduce a set of spectral measurements to a smaller number of data points which yield an optimal calibration model. In other words, they seek to extricate spectral regions which contain useful quantitative information and reject those which do not contribute substantially to an effective model. A number of methods for wavelength selection have been reported in the literature including simulated annealing,<sup>97,98</sup> genetic algorithms,<sup>99–101</sup> and iterative methods based on response variance.<sup>88</sup> In Figure 8, an example of the latter technique is presented. Shown are a typical raw spectrum, the Fourier filtered spectrum, and the wavelengths identified by the algorithm (heavy-set regions) as being most useful for prediction of glucose concentration. Raw input spectra are first Fourier filtered to remove noise and offsets. The resulting spectra are then fed into an iterative program which sequentially selects wavelengths which show largest variance and uses each in a PLS regression model. The

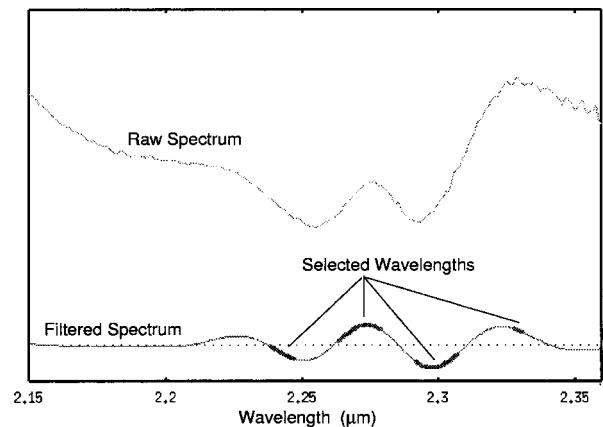


**Fig. 8** Wavelength selection for NIR spectra. After Fourier filtering of the raw NIR absorption spectrum, an iterative wavelength selection algorithm determines wavelengths which are most useful for prediction. Adapted from Ref. 88.

prediction statistics are used to determine the point at which no additional helpful information is available.

It is important to mention that iterative selection of digital filters for spectral preprocessing, wavelength selection routines, and the generation of the PLS model itself are extremely computation intensive. Exploration of the many permutations of preprocessing, selection, and calibration has only recently become possible with the arrival of readily available high-end computing power.

## 8 Conclusions

Over the last thirty years, significant efforts have been expended toward the development of an optical glucose sensor which still has not materialized. This continued enthusiasm in the face of a problem which has turned out to be exceedingly complicated is no doubt a reflection of the incredible benefits of such a sensor, namely, that it holds the potential to be fast, nonconsumable, and noninvasive in nature. While such a sensor is still at least several years from reality, the progress which has been made is very real. Chemometric methods originally developed for other applications have matured into viable tools for analysis of spectroscopic data from complex biological media. This maturation is due not only to continued experience with these tools, but to the availability of the increased computing power needed to explore the many possible permutations of their application. Simultaneously, the proliferation of optical technology in other fields continues to result in improvements in instrumentation which will eventually make optical glucose sensing possible. A noninvasive glucose sensor for diabetic home monitoring is one important application for an optical glucose sensor, however it is likely that the somewhat simpler problem of glucose sensing in other biological matrices like cell culture media will probably come to bear first. We also expect that the first optical glucose sensors for diabetic monitoring will serve as adjunct sensors whose reliability will still be routinely verified by traditional glucose measurements. Nonetheless, given the strides in methodology, instrumentation, and understanding of the problem to be faced, it is likely that a noninvasive optical glucose sensor may well exist within the next twenty years. Furthermore, it is reasonable to expect that more than one optical approach will result in a successful sensor.

## Acknowledgments

The authors wish to thank Mike McShane, Christopher Lewis, and Ashok Gowda for their assistance in preparing this manuscript, and gratefully acknowledge financial support from the Whitaker Foundation, NASA, and the National Institutes of Health.

## References

- National Institute of Diabetes and Digestive and Kidney Disorders. "The Diabetes Control and Complications Trial," NIH Publication, (1993).
- S. Blakeslee, "Doctors Announce Way to Forestall Effect of Diabetes," *The New York Times*, New York, (1993).
- I. Amato, "Race quickens for nonstick blood monitoring technology," *Science* **258**(6), 892–3 (1992).
- D. C. Klonoff, "Noninvasive blood glucose monitoring," *Diabetes Care* **20**(3), 433–7 (1997).
- J. N. Roe and B. R. Smoller, "Bloodless glucose measurements," *Critical Reviews in Therapeutic Drug Carrier Systems*, **15**(3), 199–241 (1998).
- J. D. Kruse-Jarres, "Physiochemical determination of glucose in vivo," *J. Clin. Chem. Biochem.* **26**(4), 201–8 (1998).
- O. S. Khalil, "Spectroscopic and clinical aspects of noninvasive glucose measurement," *Clin. Chem.* **45**(2), 165–77 (1999).
- P. Bhandare, Y. Mendelson, R. A. Peura, G. Jantsch, J. D. Kruse-Jarres, R. Marbach, and H. M. Heise, "Multivariate determination of glucose in whole blood using partial least-squares and artificial neural networks based on midinfrared spectroscopy," *Appl. Spectrosc.* **47**(8), 1214–21 (1993).
- M. R. Robinson, R. P. Eaton, D. M. Haaland, G. W. Koepp, E. V. Thomas, B. R. Stallard, and P. L. Robinson, "Noninvasive glucose monitoring in diabetic patients: A preliminary evaluation," *Clin. Chem.* **38**(9), 1618–22 (1992).
- R. P. Schwartz, T. J. Goodwin, and D. A. Wolf, "Cell culture for three-dimensional modeling in rotating-wall vessels: An application of simulated microgravity," *J. Tissue Culture Methods* **14**, 51–8 (1992).
- T. J. Goodwin, T. L. Prewett, D. A. Wolf, and G. F. Spaulding, "Reduced shear stress: A major component in the ability of mammalian tissue to form three-dimensional assemblies in simulated microgravity," *J. Cell. Biochem.* **51**, 301–11 (1993).
- B. G. Osbourne and T. Fearn, *Near Infrared Spectroscopy in Food Analysis*, Longman Scientific and Technical, Harlow, Essex, England (1986).
- Spectral Methods in Food Analysis*, M. M. Mossoba, Ed., Marcel Dekker, New York (1998).
- "Non/Minimally Invasive Measurement of Physiological Analytes," Proceedings Report from JDF/NASA Sponsored Technology Workshop, Washington, D.C., 7–8 April 1998 (unpublished).
- "Insulin Dependent Diabetes," National Institutes of Health Publication No. 90-2098, April (1990).
- F. Zeller, P. Novak, and R. Landgraf, "Blood glucose measurement by infrared spectroscopy," *Int. J. Artif. Organs* **12**(2), 129–35 (1989).
- P. Bhandare, Y. Mendelson, E. Stohr, and R. Peura, "Glucose Determination in Simulated Plasma Solutions Using Infrared Spectrophotometry," *Proc. IEEE* **14**, 163–4 (1992).
- H. M. Heise, R. Marbach, G. Janatsch, and J. D. Kruse-Jarres, "Multivariate determination of glucose in whole blood by attenuated total reflection infrared spectroscopy," *Anal. Chem.* **61**, 2009–15 (1989).
- K. Robinson, "Blood analysis: Noninvasive methods hover on horizon," *Biophotonics International* **5**(3), 48–52 (1998).
- W. Kaye, "Near-infrared spectroscopy: A review, Part I: Spectral identification and analytical applications," *Spectrochim. Acta* **6**, 257–87 (1954).
- E. B. Wilson, Jr., J. C. Decius, and P. C. Cross, *Molecular Vibrations: The Theory of Infrared and Raman Vibrational Spectra*, Dover, New York (1955).
- D. A. Burns and E. W. Ciurczak, *Handbook of Near-Infrared Analysis*, Marcel Dekker, New York (1992).
- R. D. Rosenthal, L. N. Paynter, and L. H. Mackie, "Noninvasive measurement of blood glucose," US Patent No. 5,028,787 (1991).
- K. Danzer, C. Fischbacher, K. U. Jagemann, and K. J. Reichelt, "Near-infrared diffuse reflection spectroscopy for noninvasive blood-glucose monitoring," *IEEE-LEOS Newsletter* **12**(2), 9–11 (1998).
- D. M. Haaland, M. R. Robinson, G. W. Koepp, E. V. Thomas, and R. P. Eaton, "Reagentless near-infrared determination of glucose in whole blood using multivariate calibration," *Appl. Spectrosc.* **46**(10), 1575–8 (1992).
- R. Marbach, T. Koschinsky, F. A. Gries, and H. M. Heise, "Noninvasive blood glucose assay by near-infrared diffuse reflectance spectroscopy of the human inner lip," *Appl. Spectrosc.* **47**(7), 875–81 (1993).
- M. A. Arnold and G. W. Small, "Determination of physiological levels of glucose in an aqueous matrix with digitally filtered Fourier transform near-infrared spectra," *Anal. Chem.* **62**, 1457–64 (1990).
- G. W. Small, M. A. Arnold, and L. A. Marquardt, "Strategies for coupling digital filtering with partial least-squares regression: Application to the determination of glucose plasma by Fourier transform near-infrared spectroscopy," *Anal. Chem.* **65**, 3279–89 (1993).
- K. H. Hazen, M. A. Arnold, and G. W. Small, "Measurement of glucose and other analytes in undiluted human serum with NIR transmission spectroscopy," *Anal. Chim. Acta* **371**, 255–267 (1998).
- K. H. Hazen, M. A. Arnold, and G. W. Small, "Temperature-

- insensitive near-infrared spectroscopic measurement of glucose in aqueous solutions," *Appl. Spectrosc.* **48**(4), 477–83 (1994).
31. P. Shengtian, H. Chung, and M. A. Arnold, "Near-infrared spectroscopic measurement of physiological glucose levels in variable matrices of protein and triglycerides," *Anal. Chem.* **68**, 1124–35 (1996).
  32. H. Chung, M. A. Arnold, M. Rhiel, and D. W. Murhammer, "Simultaneous measurements of glucose, glutamine, ammonia, lactate, and glutamate in aqueous solutions by near-infrared spectroscopy," *Appl. Spectrosc.* **50**(2), 270–6 (1996).
  33. M. J. Mattu, G. W. Small, and M. A. Arnold, "Application of multivariate calibration techniques to quantitative analysis of bandpass-filtered Fourier transform infrared interferogram data," *Appl. Spectrosc.* **51**(9), 1369–76 (1997).
  34. M. J. McShane and G. L. Coté, "Near-infrared spectroscopy for determination of glucose, lactate, and ammonia in cell culture media," *Appl. Spectrosc.* **52**(8), 1073–8 (1998).
  35. H. M. Heise, "Diffuse reflectance near-infrared spectrometry for noninvasive blood glucose monitoring," *IEEE-LEOS Newsletter* **12**(2), 11–13 (1998).
  36. P. Sabatini, "Biocontrol's diabetes monitor still faces hurdles," Pittsburgh Post-Gazette, 13 November 1999, Via Knight-Ridder/Tribune Business News via Individual Inc., Burlington MA (unpublished).
  37. E. Lanza and B. W. Li, "Application for near infrared spectroscopy for predicting the sugar content of fruit juices," *J. Food. Sci.* **49**, 995–8 (1984).
  38. C. A. Browne and F. W. Zerban, *Physical and Chemical Methods of Sugar Analysis*, 3rd ed., Wiley, New York (1941).
  39. M. J. Goetz, Jr., *Microdegree Polarimetry for Glucose Detection*, MS Thesis, University of Connecticut, Storrs, CT (1992).
  40. E. J. Gillham, "A high-precision photoelectric polarimeter," *J. Sci. Instrum.* **34**, 435–9 (1957).
  41. J. W. Gilbert, H. C. Weiser, and F. P. Holladay, "A cerebrospinal fluid glucose biosensor for diabetes mellitus," *ASAIO J.* **38**, 82–7 (1992).
  42. G. L. Coté, M. D. Fox, and R. B. Northrup, "Noninvasive optical glucose sensing using a true phase measurement technique," *IEEE Trans. Biomed. Eng.* **39**(7), 752–6 (1992).
  43. G. L. Coté, M. D. Fox, and R. B. Northrup, "Optical glucose sensor apparatus and method," US Patent No. 5,209,231, May 11, 1993.
  44. G. L. Coté, "Noninvasive optical glucose sensing—An overview," *J. Clin. Eng.* **22**(4), 253–9 (1997).
  45. S. Pohjola, "The glucose content of the aqueous humor in man," *Acta Ophthalmol. Suppl.* **88**, 11–80 (1966).
  46. W. March, R. Engerman, and B. Rabinovitch, "Optical monitor of glucose," *ASAIO Trans.* **25**, 28–31 (1979).
  47. W. March, B. Rabinovitch, and L. Adams, "Noninvasive glucose monitoring of the aqueous humor of the eye: Part II. Animal studies and the scleral lens," *Diabetes Care.* **5**(3), 259–65 (1982).
  48. C. Chou, C.-Y. Han, W.-C. Kuo, Y.-C. Huang, C.-M. Feng, and J.-C. Shyu, "Noninvasive glucose monitoring *in vivo* with an optical heterodyne polarimeter," *Appl. Opt.* **37**(16), 3553–7 (1998).
  49. B. D. Cameron and G. L. Coté, "Noninvasive glucose sensing utilizing a digital closed-loop polarimetric approach," *IEEE Trans. Biomed. Eng.* **44**(12), 1221–7 (1997).
  50. G. L. Coté and B. D. Cameron, "Noninvasive polarimetric measurement of glucose in cell culture media," *J. Biomed. Opt.* **2**(3), 275–81 (1997).
  51. T. W. King, G. L. Coté, R. J. McNichols, and M. J. Goetz, Jr., "Multispectral polarimetric glucose detection using a single pockels cell," *Opt. Eng.* **33**(8), 2746–53 (1994).
  52. R. J. McNichols, G. L. Coté, M. J. Goetz, Jr., and T. W. King, "Linear superposition of specific rotation for the detection of glucose," *Proc. IEEE* **5**(3), 1549–1550 (1993).
  53. S. P. Kozaitis, F. M. Ham, G. M. Cohen, and G. Han, "Laser polarimetry for measurement of drugs in the aqueous humor," *Proc. IEEE* **13**, 1570–1 (1991).
  54. G. L. Coté, H. Gorde, J. Janda, and B. D. Cameron, "Multispectral polarimetric system for glucose monitoring," Presented at the SPIE-BIOS, San Jose, CA, January, 1998 (unpublished).
  55. R. J. McNichols and G. L. Coté, "Development of a noninvasive polarimetric glucose sensor," *IEEE-LEOS Newsletter* **12**(2), 30–1 (1998).
  56. P. R. Carey, *Biochemical Applications of Raman and Resonance Raman Spectroscopies*, Academic Press, New York (1982).
  57. A. Mahadevan-Jansen and R. Richards-Kortum, "Raman spectroscopy for the detection of cancers and precancers," *J. Biomed. Opt.* **1**(1), 31–70 (1996).
  58. J. P. Wickstead, R. J. Erckens, M. Motamedi, and W. F. March, "Monitoring of aqueous humor metabolites using Raman spectroscopy," *Proc. SPIE* **2135**, 264–74 (1994).
  59. R. V. Tarr, *The Noninvasive Measure of D-Glucose in the Aqueous Humor of the Eye Using Stimulated Raman Spectroscopy*, PhD Dissertation, Georgia Institute of Technology, Atlanta, GA, 1991.
  60. R. V. Tarr and P. G. Steffes, "Noninvasive blood glucose measurement system and method using stimulated Raman spectroscopy," US Patent No. 5,243,983, September 14, 1993.
  61. S. Y. Wang, C. E. Hasty, P. A. Watson, J. P. Wickstead, R. D. Stith, and W. F. March, "Analysis of metabolites in aqueous humor solution by using laser Raman spectroscopy," *Appl. Opt.* **32**(6), 925–929 (1993).
  62. M. J. Goetz, Jr., G. L. Coté, R. Erckens, and W. F. March, "Application of multivariate technique to Raman spectra for quantification of body chemicals," *IEEE Trans. Biomed. Eng.* **42**(7), 728–31 (1995).
  63. A. J. Berger, I. Itzkan, and M. S. Feld, "Feasibility of measuring blood glucose concentration by near infrared Raman spectroscopy," *Spectrochim. Acta A* **53**(2), 287–92 (1997).
  64. J. Lambert, M. Storrie-Lombardi, and M. Borchert, "Measurement of physiological glucose levels using Raman spectroscopy in a rabbit aqueous humor model," *IEEE-LEOS Newsletter* **12**(2), 19–22 (1998).
  65. X. Dou, Y. Yamaguchi, H. Yamamoto, S. Doi, and Y. Ozaki, "A highly sensitive, compact Raman system without a spectrometer for quantitative analysis of biological samples," *Vib. Spectrosc.* **14**(2), 199–205 (1997).
  66. R. V. Tarr and P. G. Steffes, "The noninvasive measure of D-glucose in the ocular aqueous humor using stimulated Raman spectroscopy," *IEEE-LEOS Newsletter* **12**(2), 22–27 (1998).
  67. A. J. Berger, T. W. Koo, I. Itzkan, and M. S. Feld, "An enhanced algorithm for linear multivariate calibration," *Anal. Chem.* **70**(3), 623–7 (1998).
  68. C. H. Spiegelman, M. J. McShane, M. J. Goetz, M. Motamedi, Q. L. Yue, and G. L. Coté, "Theoretical justification of wavelength selection in PLS calibration: Development of a new algorithm," *Anal. Chem.* **70**(1), 35–44 (1998).
  69. B. P. Schaffar and O. S. Wolfbeis, "A fast responding fiber optic glucose biosensor based on an oxygen optrode," *Biosens. Bioelectron.* **5**(2), 137–48 (1990).
  70. M. C. Moreno-Bondi, O. S. Wolfbeis, M. J. Leiner, and B. P. Schaffar, "Oxygen optrode for use in a fiber-optic glucose biosensor," *Anal. Chem.* **62**(21), 2377–80 (1990).
  71. Z. Rosenzweig and R. Kopelman, "Analytical properties and sensor size effects of a micrometer-sized optical fiber glucose biosensor," *Anal. Chem.* **68**(8), 1408–13 (1996).
  72. L. Li and D. R. Walt, "Dual-analyte fiber-optic sensor for the simultaneous and continuous measurement of glucose and oxygen," *Anal. Chem.* **67**, 3746–53 (1995).
  73. H. Gunsingham, C.-H. Tan, and J. K. L. Seow, "Fiber-optic glucose sensor with electrochemical generation of indicator reagent," *Anal. Chem.* **62**, 755–59 (1990).
  74. M. S. Abdel-Latif and G. G. Guilbault, "Fiber-optic sensor for the determination of glucose using micellar enhanced chemiluminescence of the peroxyate reaction," *Anal. Chem.* **60**, 2671–4 (1988).
  75. J. S. Schultz, S. Mansouri, and I. J. Goldstein, "Affinity sensor: A new technique for developing implantable sensors for glucose and other metabolites," *Diabetes Care.* **5**(3), 245–253 (1982).
  76. S. Mansouri and J. S. Schultz, "A miniature optical glucose sensor based on affinity binding," *Biotechnology*, 885–90 (1984).
  77. D. L. Meadows and J. S. Schultz, "Design, manufacture, and characterization of an optical fiber glucose affinity sensor based on a homogeneous fluorescence energy transfer Assay system," *Anal. Chim. Acta* **280**, 21–30 (1993).
  78. R. Ballerstadt and J. S. Schultz, "Competitive-binding Assay method based on fluorescence quenching of ligands held in close proximity by a multivalent receptor," *Anal. Chim. Acta* **345**, 203–12 (1997).
  79. J. R. Lakowicz and B. Maliwal, "Optical sensing of glucose using phase-modulation fluorimetry," *Anal. Chim. Acta* **271**, 155–64 (1993).
  80. L. Tolosa, H. Szmazinski, G. Rao, and J. R. Lakowicz, "Lifetime-based sensing of glucose using energy transfer with a long lifetime donor," *Anal. Biochem.* **250**, 102–8 (1997).

81. *Computerized Quantitative Infrared Analysis*, G. L. McClure, Ed., American Society of Testing and Materials, Philadelphia, PA (1987).
82. H. Martens and T. Næs, *Multivariate Calibration*, Wiley, New York (1989).
83. D. M. Haaland and E. V. Thomas, "Partial least-squares methods for spectral analyses. 1. relation to other quantitative calibration methods and the extraction of qualitative information," *Anal. Chem.* **60**, 1193–1202 (1988).
84. G. Brown, "An optimization criterion for linear inverse estimator," *Technometrics* **21**, 575–9 (1979).
85. H. Wold, "Soft modeling: The basic design and some extensions," in *Systems Under Indirect Observation, Causality-Structure-Prediction*, K. G. Jöreskog and H. Wold, Eds. North Holland, Amsterdam (1981).
86. S. J. Leon, *Linear Algebra with Applications*, 3rd ed., MacMillan, New York (1990).
87. P. J. Brown, C. H. Spiegelman, and M. C. Denham, "Chemometrics and spectral frequency selection," *Philos. Trans. R. Soc. London, Ser. A* **337**, 311–22 (1991).
88. M. J. McShane, G. L. Coté, and C. H. Spiegelman, "Variable selection in multivariate calibration of a spectroscopic glucose sensor," *Appl. Spectrosc.* **51**(10), 1559–64 (1997).
89. H. M. Heise and A. Bittner, "Multivariate calibration for near-infrared spectroscopic Assays of blood substrates in human plasma based on variable selection using PLS-regression vector choices," *Fresenius J. Anal. Chem.* **362**(1), 141–7 (1998).
90. P. Geladi, D. McDougall, and H. Martens, "Linearization and scatter-correction for near-infrared reflectance spectra of meat," *Appl. Spectrosc.* **39**(3), 491–500 (1985).
91. S. Pan, H. Chung, and M. A. Arnold, "Near-infrared spectroscopic measurement of physiological glucose levels in variable matrices of protein and triglycerides," *Anal. Chem.* **68**, 1124–35 (1996).
92. G. Lu, X. Zhou, M. A. Arnold, and G. W. Small, "Multivariate calibration models based on the direct analysis of near-infrared single-beam spectra," *Appl. Spectrosc.* **51**(9), 1330–9 (1997).
93. F. M. Ham, I. N. Kostanic, G. M. Cohen, and B. R. Gooch, "Determination of glucose concentrations in an aqueous matrix from NIR spectra using optimal time-domain filtering and partial least-squares," *IEEE Trans. Biomed. Eng.* **44**(6), 475–85 (1997).
94. R. E. Schaffer, G. W. Small, and M. A. Arnold, "Genetic algorithm-based protocol for coupling digital filtering and partial least-squares regression: Application to the near-infrared analysis of glucose in biological matrices," *Anal. Chem.* **68**, 2663–75 (1996).
95. W. F. McClure, A. Hamid, F. G. Giesbrecht, and W. W. Weeks, "Fourier analysis enhances NIR diffuse reflectance spectroscopy," *Appl. Spectrosc.* **38**(3), 322–9 (1984).
96. A. Gowda and R. J. McNichols, SBIR Program Final Report, NIH Grant No. 01-R43-DK53718-01 (1998).
97. U. Hörchner and J. H. Kalivas, "Further investigation on a comparative study of simulated annealing and genetic algorithm for wavelength selection," *Anal. Chim. Acta* **311**, 1–13 (1995).
98. J. H. Kalivas, N. Roberts, and J. M. Sutter, *Anal. Chem.* **68**, 2024–30 (1996).
99. C. B. Lucasius, M. L. M. Beckers, and G. Kateman, "Genetic algorithms in wavelength selection: A comparative study," *Anal. Chim. Acta* **286**, 135–53 (1994).
100. D. Jouan-Rimbaud and D-L. Massart, "Genetic algorithms as a tool for wavelength selection in multivariate calibration," *Anal. Chem.* **67**, 4295–4301 (1995).
101. A. S. Bangalore, R. E. Shaffer, and G. W. Small, "Genetic algorithm-based method for selecting wavelengths and model size for use with partial least-squares regression: Application to near-infrared spectroscopy," *Anal. Chem.* **68**, 4200–12 (1996).